Geomechanics and Engineering, *Vol. 41, No. 4 (2025) 443-453*
https://doi.org/10.12989/gae.2025.41.4.443

Active earth thrust on vertical walls supporting sandy sloping ground of different height and toe position

Sunil Khuntia[1a] and Jagdish Prasad Sahoo*[2]

[1]*Department of Civil Engineering, National Institute of Technology Rourkela 769008, India*
[2]*Department of Civil Engineering, Indian Institute of Technology Kanpur 208016, India*

(*Received July 21, 2023, Revised April 12, 2025, Accepted May 7, 2025*)

Abstract. The present study evaluates the active earth thrust exerted by sandy sloping ground on rigid retaining walls, investigating the critical effects of slope toe position (e) and slope height (h) that are often neglected in current design standards despite their significant influence on wall pressures. The solutions were obtained by performing finite element lower bound limit analysis with second order conic optimization techniques and presented in the form of non-dimensional earth pressure coefficient (K_a). The active earth thrust remains constant beyond a certain distance of slope toe from the back face wall, and height of slope, which are defined as critical toe distance (e_{cr}) and critical slope height (h_{cr}), respectively. The critical toe distance and slope height have been found to be influenced by the friction angle of soil (ϕ), inclination of slope (β) and surcharge pressure (q) on the ground surface. The study shows that the magnitudes of K_a, e_{cr}, and h_{cr} increase with a reduction in the values of ϕ and with an increase in the values of β and q. For a few typical cases, the proximity of stress state to failure was presented.

Keywords: active thrust; finite elements; limit analysis; retaining wall; sand; slope

1. Introduction

Retaining walls are usually constructed to support the soil and keep a difference in the elevation of the ground surface due to the unavailability of sufficient space to provide appropriate side slopes for the construction of roads, highways, and buildings along cuts and fills. The stability of these walls depends on the active earth thrust exerted by the supported/backfill soil. The active thrust depends on the properties of backfill soil, surcharge pressure on the backfill, inclination, and height of backfill, and position of the toe of the sloping backfill. Many research works have already been performed to determine the active earth thrust on retaining walls. Based on the limit equilibrium concept with the consideration of a triangular rigid wedge of backfill at failure, Coulomb (1776) first developed theoretical solutions for determining the active earth thrust on rigid retaining walls with rough back surfaces. Rankine (1857) proposed a theory for calculating the active earth pressure considering a small soil element at failure of the backfill for smooth wall-soil interface conditions. Active earth pressure on a retaining wall considering the influence of self-weight, cohesion and friction angle of soil, surcharge pressure and backfill inclination, various solutions have been developed based on limit equilibrium and limit analysis theories (Terzaghi 1943, Jumikis 1962, Chen and Rosenfarb 1973, Kérisel and Absi 1990, Soubra and Macuh 2002). The magnitude of active earth forces due to line surcharge and uniformly distributed surcharge of infinite and finite lengths acting at distances from the wall has been computed by adopting Coulomb's rigid wedge planar mechanism (Motta 1994, Greco 2005, 2006). Fan and Fang (2010) obtained numerical solutions for computing active earth pressures on rigid retaining walls with limited backfill space owing to the existence of rock face employing finite element analysis. By carrying out two-dimensional finite difference analyses with the usage of the Fast Lagrangian Analysis of Continua Code (FLAC), Benmeddour *et al.* (2012) computed the active earth pressure coefficients of cohesionless sloping backfill by varying the position of slope toe from the top of wall. Like the problem tackled by Fan and Fang (2010), Greco (2013) provided closed-form solutions for evaluating the active thrust on gravity retaining walls with narrow backfill by extending classical earth pressure theory of Coulomb based on limit equilibrium method. Fang *et al.* (1997) reported experimental results on earth pressure acting against a vertical rigid wall subjected to translational movements with sloping cohesionless backfill having an inclination angle of 20°, unit weight of 15.5 kN/m3, soil friction angle of 30.9° and soil-wall interface friction angle of 19.2°. A series of experimental studies were carried out by Yang and Tang (2017) to study the active earth pressure on retaining walls for three different wall movement modes and different backfill widths. Implementing upper bound theorem of limit analysis, Sahoo and Ganesh (2017) derived the expression for K_a with the inclined wall and sloping backfill in the presence of seismic loading and surcharge load for cohesive-frictional soil. Using finite element numerical technique, Lai *et al.* (2022) have recently studied the failure mechanisms of retaining walls with narrow cohesive-

*Corresponding author, Associate Professor
E-mail: jpsahoo@iitk.ac.in
[a]Ph.D.

ISSN: 2005-307X (Print), 2092-6219 (Online)

Table 1 Summary of methodology adopted by various researchers

Methodology	References
Numerical Simulation	Fan and Fang (2010), Benmeddour *et al*. (2012), Greco (2013), Lai *et al*. (2022)
Theoretical Derivation	Coulomb (1776), Rankine (1857), Jumikis (1962), Rosenfarb (1973), Kerisel and Absi (1990), Chen and Motta (1994), Soubra and Macuh (2002), Greco (2005, 2006), Yang and Tang (2017), Sahoo and Ganesh (2018)
Experimental Verification	Fang *et al.* (1997), Yang and Tang (2017)

frictional soil backfill. Table 1 provides a systematic classification of the methodological approaches (numerical, theoretical, and experimental) used in the literature.

Except the study of Benmeddour *et al.* (2012) and Sahoo and Ganesh (2018), no works seem to have been performed for examining the influence of distance of slope toe from the wall, where the height of the slope is assumed to be very high (can be said as infinite slope). However, in the case of sloping ground, the height of the slope is found to be limited (finite slopes). Hardly any research work has been reported for computing the active earth force on walls retaining sloping ground of limited height. In the present analysis, by employing lower bound finite element limit analysis and second order conic optimization techniques, numerical solutions have been obtained for estimating the active earth force on rigid retaining walls supporting sandy soil with the sloping surface (i) whose toe is located at different distances from the back face of the wall, and (ii) of different heights above the top of the wall. The effect of the inclination of the slope, soil friction angle, and the ground surcharge has been examined. Few typical cases have been taken into consideration to examine the failure patterns.

2. Statement of the problem

A rigid retaining wall of height H retaining an infinite and finite height sandy sloping ground is shown in Figs. 1(a) and 1(b), respectively, where toe is located at a distance 'e' from the back face wall. In the case of an infinite slope, the height of the slope is very high, or the crest is located at a height beyond which further increase in height negligibly influences the failure mechanism or earth pressure distribution; thus, the crest is not shown. Whereas in the case of the finite slope, h is the height of the crest/slope above the top of the wall that actively modifies the failure surface and wall pressures. The angle of the sloping surface with the horizontal plane is β, and a uniform surcharge pressure of magnitude q is acting on the ground surface.

The soil mass is assumed to be perfectly plastic and obeys Mohr–Coulomb failure criterion with an associated flow rule. The angle of internal friction and unit weight of soil are denoted as ϕ and γ, respectively. For performing plane strain analysis, the length of wall is considered very long as compared to its height. The magnitude of active force (P_a) per unit length of wall is intended to be determined.

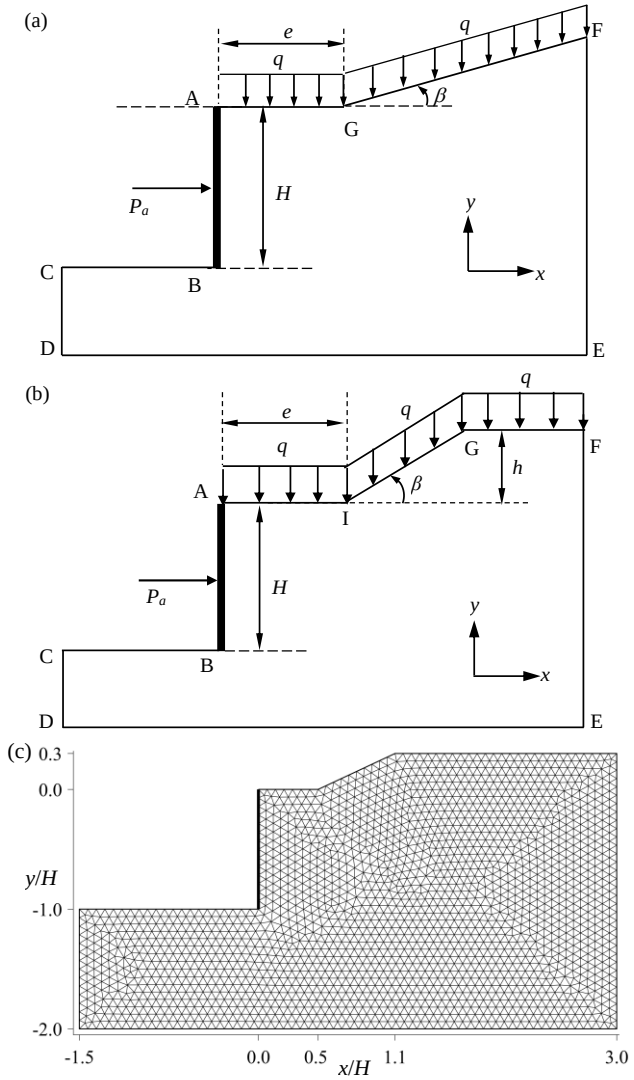

Fig. 1 (a) an infinite height sloping ground with toe at a distance 'e' from wall ; and (b) a finite height sloping ground with toe at a distance 'e' from wall; and (c) a typical finite element mesh for e/H = 0.5 and h/H = 0.3

3. Analysis

Finite Element Limit Analysis (FELA) offers advantages over traditional methods by combining computational efficiency with rigorous lower bound plasticity theory, eliminating the need for assumed failure mechanisms while accommodating complex soil profiles and

boundary conditions. With application of finite element analysis based on lower bound theorem of limit analysis as formulated by Sloan (1988) and following the second order conic optimization procedure proposed by Makrodimopoulos and Martin (2006), the present analysis was performed for computing the active earth force on a vertical rigid retaining wall. The magnitude of collapse load at active failure (objective function) is optimized subjected to a set of constraints imposed on the unknown nodal stresses. The constraints generated for ensuring (i) the equilibrium of elements, (ii) the discontinuities are statically admissible, and (iii) the satisfaction of associated boundary stresses, are the linear equality constraints. On the other hand, inequality constraints are developed for satisfying the yield criterion.

The chosen domains as shown in Figs. 1(a) and 1(b) are discretized into a number of three noded triangular elements. For $\beta = 15°$, a typical finite element mesh for $e/H = 0.5$ and $h/H = 0.3$ is shown in Fig. 1(c). Each node is involved with three basic unknowns, namely, horizontal normal stress (σ_x), vertical normal stress (σ_y), and the shear stress (τ_{xy}) on the horizontal/vertical plane. A linear variation of stress components was considered by using linear shape functions. The following equations are required to be satisfied everywhere in the problem domain for satisfying element equilibrium condition,

$$\frac{\partial \sigma_x}{\partial x} + \frac{\partial \tau_{xy}}{\partial y} = 0 \tag{1}$$

$$\frac{\partial \tau_{xy}}{\partial x} + \frac{\partial \sigma_y}{\partial y} = \gamma \tag{2}$$

The inclusion of statically admissible stress discontinuities in the lower bound analysis provides olutions close to the true solution (Drucker 1953). The lines of discontinuities are considered at the interfaces of adjacent elements to incorporate statically admissible stress discontinuities, and the continuity of shear and normal stresses along these interfaces are allowed (Sloan 1988). The boundaries CD and DE are kept at large distance so that (i) the plastic yield points developed during the analysis are contained quite well within the chosen boundaries of the domain, and (ii) the magnitude of active force at failure remains almost unchanged with further increase in the domain size.The nodes along the ground surface AF as shown in Figs. 1(a), and AG and FE as shown in Fig. 1(b) were prescribed with vertical stresses equal to surcharge pressure, that is, $\sigma_y = q$; whereas, the nodes along the ground surface FE as given in Fig. 1(a) and GF as given in Fig. 1(b) must satisfy the following conditions

$$\sigma_x \sin^2\beta + \sigma_y \cos^2\beta - \tau_{xy} \sin 2\beta = -q\cos^2\beta \tag{3}$$

$$-\frac{1}{2}\sin 2\beta\sigma_x + \frac{1}{2}\sin 2\beta\sigma_y + \cos 2\beta\tau_{xy} = -q\sin\beta\cos\beta \tag{4}$$

No constraints are imposed on the values of stresses on the nodes along the boundaries BC, CD and DE. Assuming the wall-soil interface is smooth, the shear stresses (τ_{xy}) along the nodes AB were specified equal to zero.

The Mohr-Coulomb yield condition is ensured not to be violated in the domain. The Mohr–Coulomb failure criterion for a plane-strain problem can be expressed in following form

$$\sqrt{(\sigma_x - \sigma_y)^2 + 4\tau_{xy}^2} \le (\sigma_x + \sigma_y)\sin\phi \tag{5}$$

The nonlinear inequality constraints generated for satisfying the yield condition (Eq. (5)) is expressed as a set of second order cone constraints at each node (Makrodimopoulos and Martin 2006), which can be represented as

$$A_{soc}^{i}\sigma_i + z_i = b_{soc}^{i} \tag{6}$$

where, $A_{soc}^{i} = \begin{bmatrix} \sin\phi & \sin\phi & 0 \\ -1 & 1 & 0 \\ 0 & 0 & -2 \end{bmatrix}$; $\sigma_i = \begin{bmatrix} \sigma_{xi} \\ \sigma_{yi} \\ \tau_{xyi} \end{bmatrix}$;

$z_i = \begin{bmatrix} z_{1i} \\ z_{2i} \\ z_{3i} \end{bmatrix}$; $b_{soc}^{i} = \begin{bmatrix} 0 \\ 0 \\ 0 \end{bmatrix}$

σ_{xi}, σ_{yi} and τ_{xyi} are the the horizontal normal stress, vertical normal stress and shear stress, respectively, at i^{th} node. $z = \{z_1 \quad z_2 \quad z_3\}^T$ is a vector representing the second-order cone which satisfies $z_1 \ge \sqrt{z_2^2 + z_3^2}$.

The magnitude of active earth force (P_a) per unit length of wall can be obtained by integrating the normal stresses along the wall

$$P_a = \int \sigma_x dy \tag{7}$$

The global matrices and vectors are formed by assembling equality and inequality constraints imposed at all the nodes. The second order conic programming problem is expressed in a standard form as follows

Objective function: Maximize $\{c\}^T\{\sigma\}$ or

$$\text{Minimize } -\{c\}^T\{\sigma\} \tag{8}$$

Constraints: $[A]\{x\}=\{B\}$ (9)

where, $\{c\}$ is the global vector of objective function coefficients, $\{x\}^T = \{\sigma, z\}$, global variables consisting of unknown nodal stresses $\{\sigma\}$ and auxiliary variables $\{z\}$, $[A]$ and $\{B\}$are global matrix of coefficients and global vector of constants developed for satisfying element equilibrium, stress boundary, statically admissible stress discontinuity and yield conditions.

A necessary pre-processing computer code was generated in MATLAB (2015) for performing the analysis and conic optimization was performed by using MOSEK (2015), an optimization toolbox available for MATLAB (2015).

4. Results and discussions

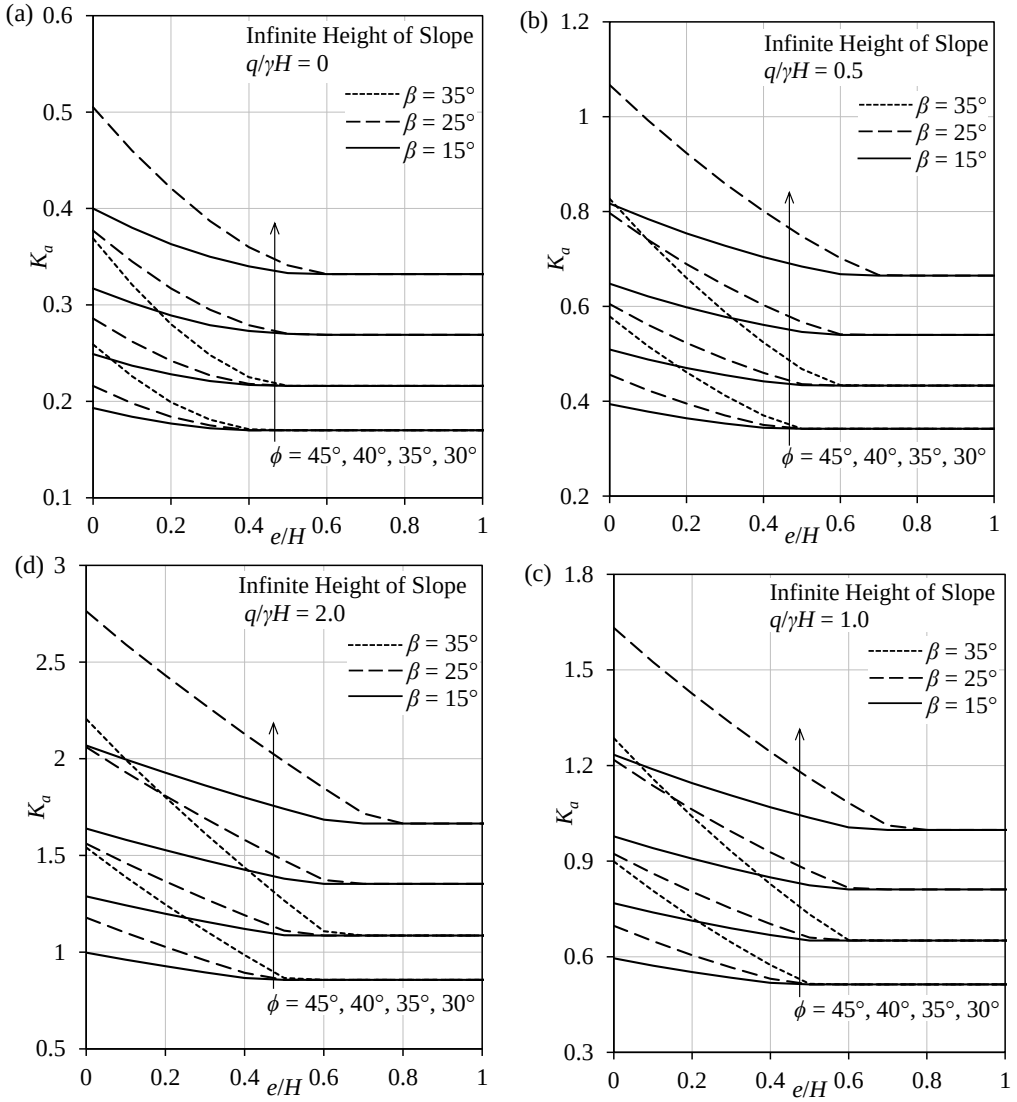

Fig. 2 For infinite height of slope, variation of K_a with e/H for different combinations of ϕ and β (a) $q/\gamma H = 0$, (b) $q/\gamma H = 0.5$, (c) $q/\gamma H = 1$; and (d) $q/\gamma H = 2$

The computations have been performed for determining the active thrust for different combinations of slope angle (β), normalized distance of slope toe (e/H) from wall, normalized height of the sloping ground (h/H), internal friction angle of soil (ϕ), normalized surcharge ($q/\gamma H$) for smooth interface of retaining wall. However, a few cases have been considered to investigate the effect of interface friction angle (δ). Extensive computations were performed by varying e/H for the case (i) when height of the sloping ground is very large (infinite slope) (ii) height of sloping ground is limited (finite slopes). The active earth force can be expressed in terms of non-dimensional earth pressure coefficient as

$$P_a = \frac{1}{2}\gamma H^2 K_a \tag{10}$$

where, K_a is active earth pressure coefficient.

The variation of K_a has been presented as a function of β, e/H, h/H, ϕ, $q/\gamma H$, δ/ϕ and results were discussed as follows.

4.1 Variation of K_a with e/H for infinite height of sloping ground

For different combinations of parameters such as β, ϕ and $q/\gamma H$, the variation of active earth pressure coefficient with e/H for infinite height of slope is shown in Figs. 2(a)-(d). with e/H for infinite height of slope is shown in Figs. 2(a)-2(d). From these figures, the magnitude of K_a is seen to be reduced with an increase in the values of e/H and remains constant beyond a certain value of e/H, which is defined as the critical value of e/H, that is, $(e/H)_{cr}$. The magnitude of active earth force corresponding to e/H greater than equal to $(e/H)_{cr}$ becomes exactly the same as

4.2 Variation of K_a with e/H for different height of sloping ground

The variation of active earth pressure coefficient with e/H for finite height of slopes is shown in Figs. 3-6. For a

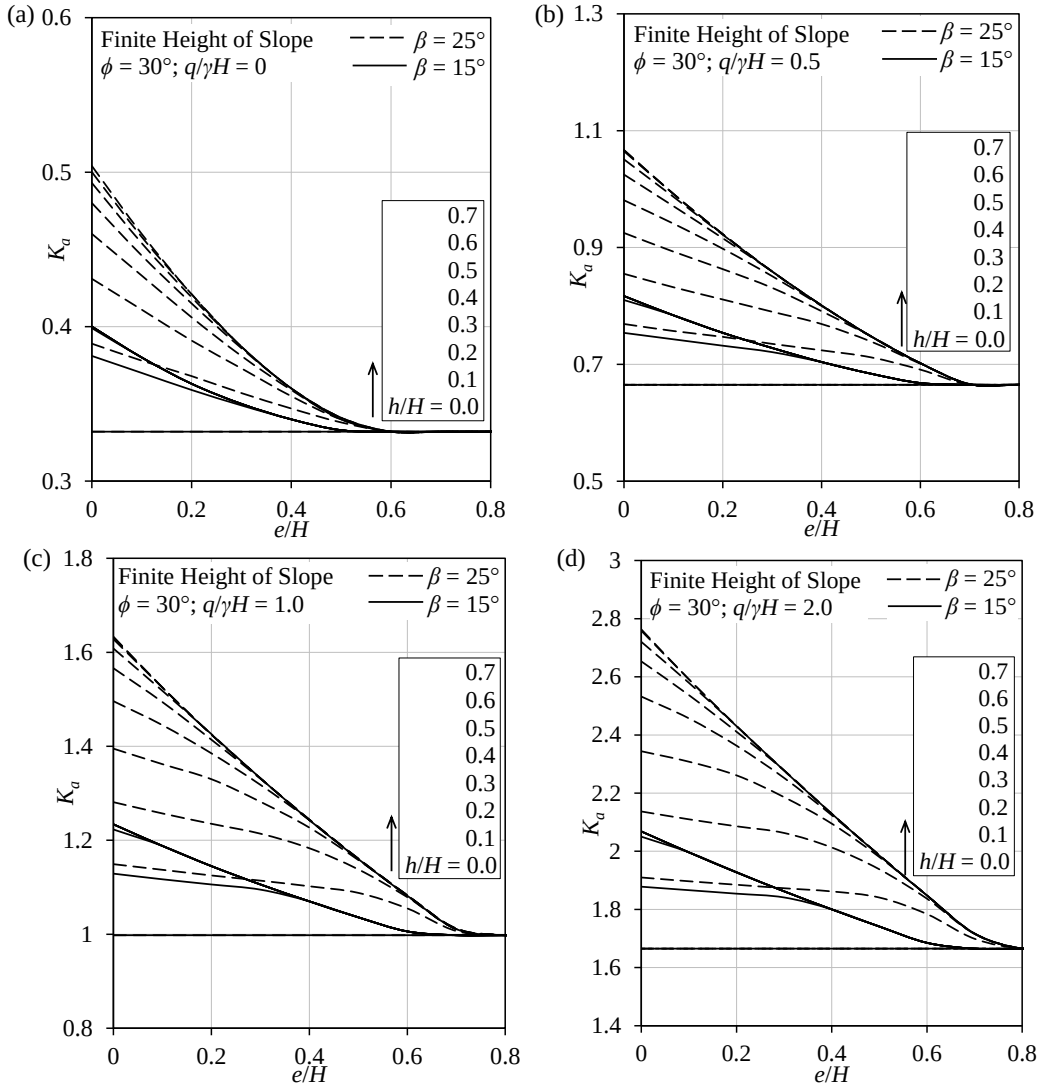

Fig. 3 For finite height of slope with ϕ = 30º, variation of K_a with e/H for different combinations of h/H and β (a) $q/\gamma H$ = 0, (b) $q/\gamma H$ = 0.5, (c) $q/\gamma H$ = 1; and (d) $q/\gamma H$ = 2

given value of e/H, the magnitude of K_a is found to be increasing as the value of h/H increases found to be increasing as the value of h/H increases and remains constant beyond a certain value of h/H, which is defined as the is defined as the critical value of h/H, that is, $(h/H)_{cr}$. By comparing the results from Fig. 2 with those in with those in Figs. 3-6, it could be noticed that the magnitude of active earth force exerted by finite sloping ground corresponding to h/H greater than equal to $(h/H)_{cr}$ becomes the same as that exerted by infinite sloping ground. Further, corresponding to a particular height of slope, the value of K_a reduces up to the critical value of e/H and remains constant after that. The magnitude of $(e/H)_{cr}$ and $(h/H)_{cr}$ are noted to be higher for lower friction angle values of soil and greater values of slope inclination and surcharge pressure increasing as the value of h/H increases and remains constant beyond a certain value of h/H, which is defined as the critical value of h/H, that is, $(h/H)_{cr}$. By comparing the results from Fig. 2 with those in Figs. 3-6, it could be noticed that the magnitude of active earth force exerted by finite sloping ground corresponding to h/H greater than equal to $(h/H)_{cr}$ becomes the same as that exerted by infinite sloping ground. Further, corresponding to a particular height of slope, the value of K_a reduces up to the critical value of e/H and remains constant after that. The magnitude of $(e/H)_{cr}$ and $(h/H)_{cr}$ are noted to be higher for lower friction angle values of soil and greater values of slope inclination and surcharge pressure However, the variation in the values of $(e/H)_{cr}$ has been found to be insignificant with change in the values of h/H. But a reduction in the critical height of slope is observed with an increase in the toe distance from the wall; for instance, the value of K_a remains the same corresponding to h/H greater than equal to 0.3, 0.2 and 0.1, when e/H is approximately equal to 0.1, 0.35 and 0.65, respectively for $q/\gamma H$ = 2, β = 15° and ϕ = 45° as shown in Fig. 6(d).

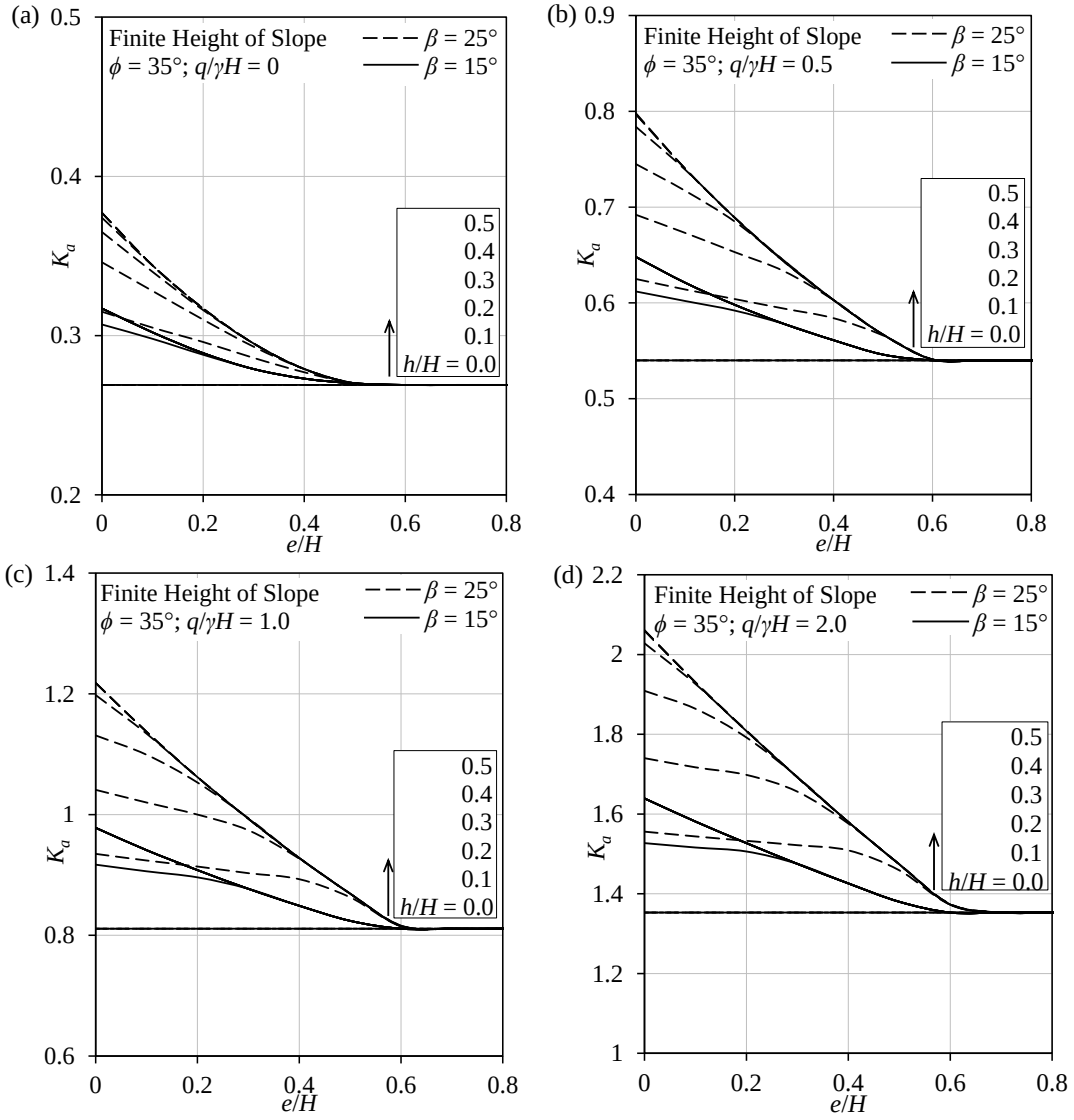

Fig. 4 For finite height of slope with ϕ = 35º, variation of K_a with e/H for different combinations of h/H and β (a) $q/\gamma H$ = 0, (b) $q/\gamma H$ = 0.5, (c) $q/\gamma H$ = 1; and (d) $q/\gamma H$ = 2

4.3 Variation of K_a with slope angle (β), soil friction angle (ϕ) and surcharge ($q/\gamma H$)

From Figs. 2-6, the magnitude of the earth pressure coefficient has been found to enhance continuously with an increase in the values of slope inclination and surcharge pressure on the ground surface and with a decrease in the values of ϕ. Further, it can be noted that the magnitude of coefficient K_a is reduced significantly for sloping ground with lower inclination , higher soil friction angle, and lower ground surcharge. It needs to be mentioned that the coefficient K_a was computed for $\beta < \phi$, as the sandy soil slopes are unstable when β is greater than equal to ϕ.

4.4 Variation of K_a with δ/ϕ for finite and infinite slope

To examine the variation of K_a with the δ/ϕ, computation has been carried out for β = 25°, $q/\gamma H$ = 0 and 1.0 with ϕ = 30° and 40° for infinite and finite slope as shown in Figs. 7(a) and 7(b) respectively. It can be clearly observed that for a smooth interface (i.e., δ/ϕ = 0), the coefficient of active earth pressure is found to be maximum, which is conservative. For all the cases, the percentage of change of K_a is found to be around 15 % to 25 % when the δ/ϕ changes from 0 to 1 (i.e., smooth to rough).

4.5 Proximity of stress state to failure

A point within the chosen domain will be in a state of shear failure when the state of stress of that point located on the Mohr's stress circle touches the Mohr-Coulomb failure envelope. The proximity of the stress state to shear failure that is failure pattern is determined in terms of ratio namely t/s where $t = (\sigma_x - \sigma_y)^2 + (2\tau_{xy})^2$; and $s = ((\sigma_x + \sigma_y)\sin\phi)^2$.the value of t/s at any point is equal to unity corresponding to ultimate shear failure, and t/s becomes smaller than unity at a point in a non-yielding state. For ϕ = 30º, β = 25° and $q/\gamma H$ = 0, the failure patterns have been generated

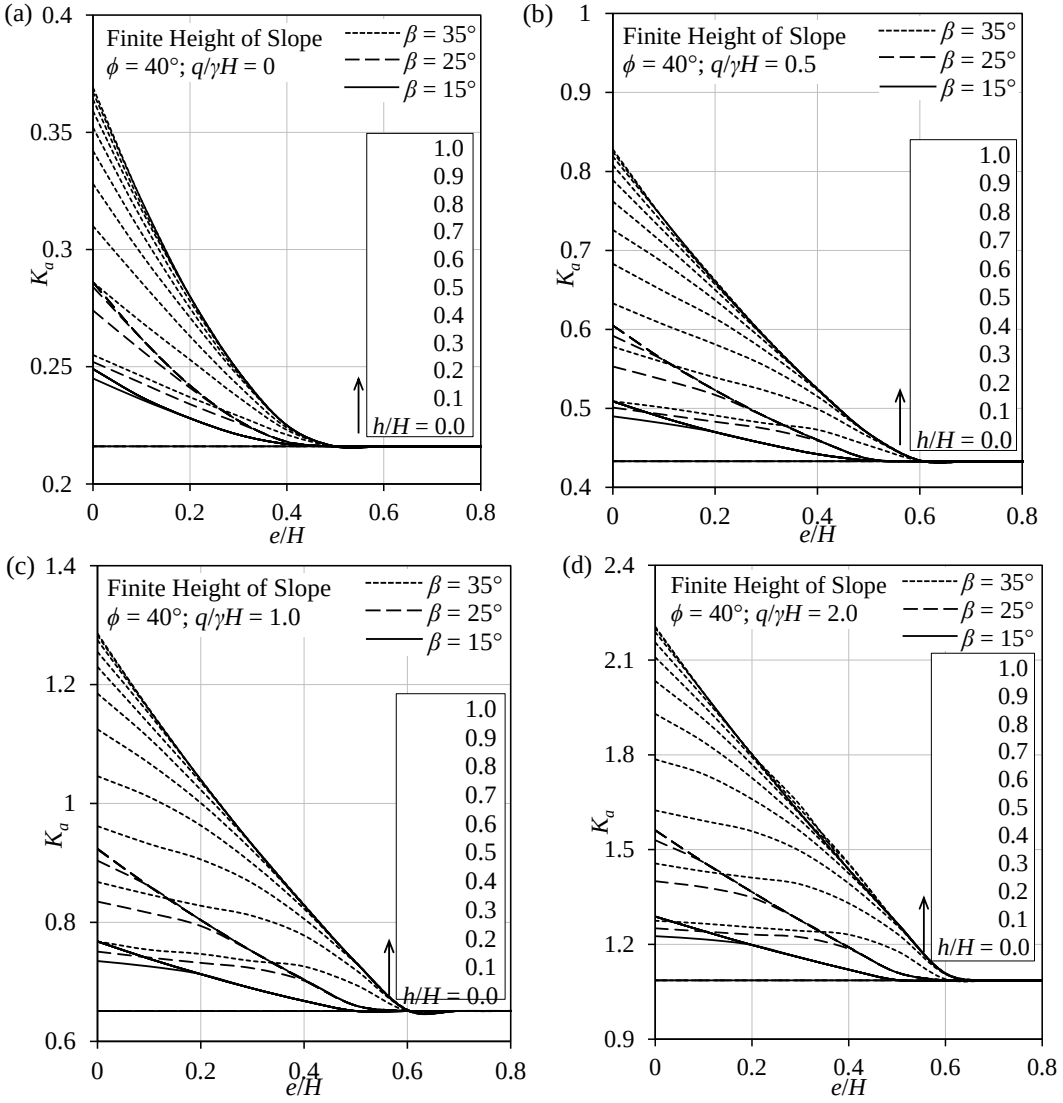

Fig. 5 For finite height of slope with ϕ = 40º**,** variation of K_a with e/H for different combinations of h/H and β (a) $q/\gamma H$ = 0, (b) $q/\gamma H$ = 0.5, (c) $q/\gamma H$ = 1; and (d) $q/\gamma H$ = 2

for (i) infinite height of slopes by varying e/H, as shown in Fig. 8, and (ii) finite height slopes by changing both e/H and h/H as illustrated in Fig. 9. From these figures, it can be noticed that the zone of yielding (dark part), that is, the mass of soil yields at the ultimate active state, becomes larger with reduction in the distance of slope toe from the wall. Figs. 9(b) and 9(c) reveal a direct correlation between slope height and yielding zone expansion at fixed toe positions, with the plastic region enlarging proportionally to height increment. Figs. 9(b) and 9(c) reveal a direct correlation between slope height and yielding zone expansion at fixed toe positions, with the plastic region enlarging proportionally to height increment. For two different values of $q/\gamma H$ in the case of finite height of slope, the proximity of stress state to failure for ϕ = 40º, β = 35°, e/H = 0 and h/H = 0.2 is shown in Fig. 10 and it can be observed that the failure zone is larger for higher values of $q/\gamma H$.

5. Validation of present numerical solutions

The validity of the numerical solutions obtained from the present analysis has been verified by comparing with those available in literature as shown in Fig. 11. Fig. 11(a) shows a comparison of variation of K_a with e/H obtained from the present analysis with that of Benmeddour *et al.* (2012) for different values of ϕ and β/ϕ. The present solutions are in good agreement with the results reported by Benmeddour *et al*. (2012) based on finite difference analyses using FLAC software. The present values of K_a are compared with the laboratory experimental results of Fang *et al.* (1997) and the theoretical solutions of Coulomb (1776) and Sahoo and Ganesh (2018) as shown in Fig. 11(b). Fang *et al*. (1997) conducted laboratory experiments for a vertical retaining wall of height 0.3 m supporting sloping backfill (β) with unit weight (γ) and internal friction angle (ϕ) of 15.5 kN/m^3 and 30.9°, respectively and the soil-wall interface (δ) friction angle was 19.2°. Solutions based on Coulomb's theory are presented using the limit

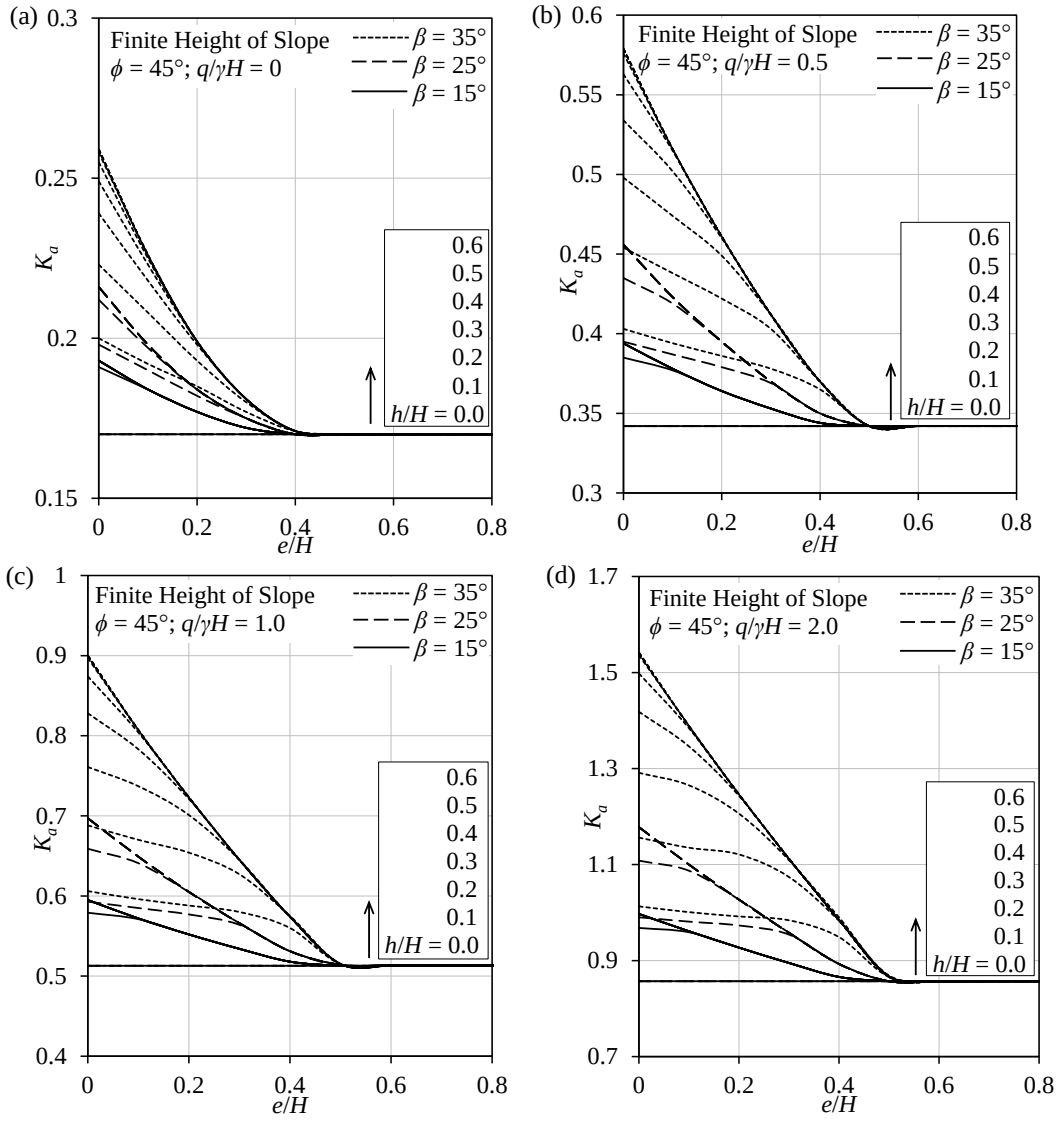

Fig. 6 For finite height of slope with ϕ = 45º, variation of K_a with e/H for different combinations of h/H and β (a) $q/\gamma H$ = 0, (b) $q/\gamma H$ = 0.5, (c) $q/\gamma H$ = 1; and (d) $q/\gamma H$ = 2

Table 2 A comparison of K_a values obtained from the present analysis with that of Soubra and Macuh (2002) for different combinations of ϕ and β/ϕ

ϕ	β/ϕ	Soubra and Macuh (2002)	Present analysis
20°	0	0.49	0.49
	1/3	0.54	0.54
	1/2	0.57	0.57
	2/3	0.61	0.61
30°	0	0.33	0.33
	1/3	0.37	0.37
	1/2	0.40	0.40
	2/3	0.44	0.44
40°	0	0.22	0.22
	1/3	0.25	0.25
	1/2	0.27	0.27
	2/3	0.30	0.30

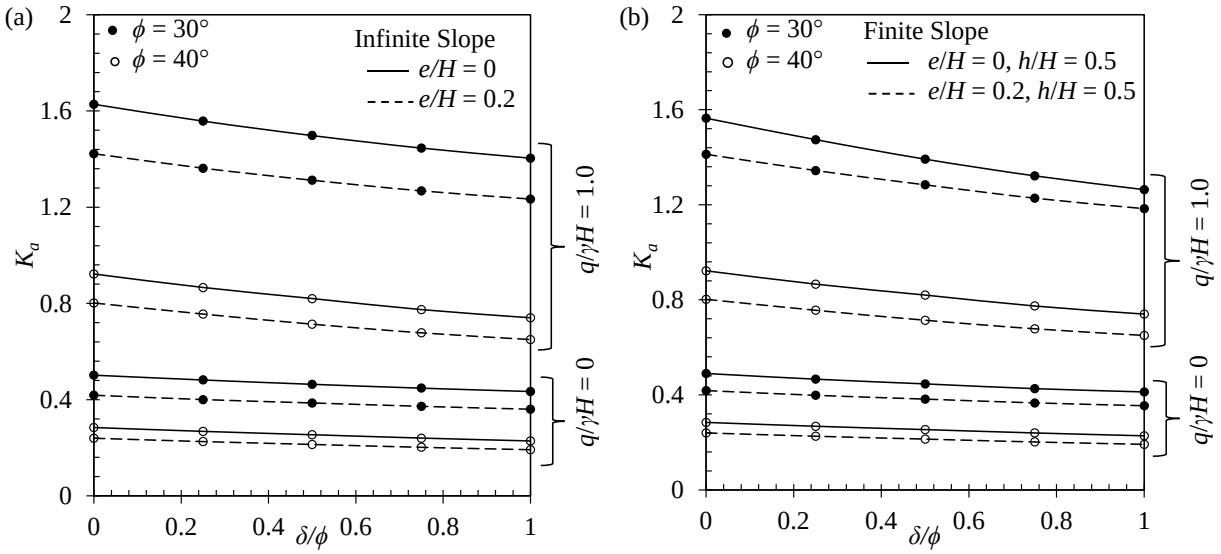

Fig. 7 **V**ariation of K_a with δ/ϕ for $\beta = 25°$ and different combinations of ϕ and $q/\gamma H$ (a) Infinite slope and (b) Finite slope

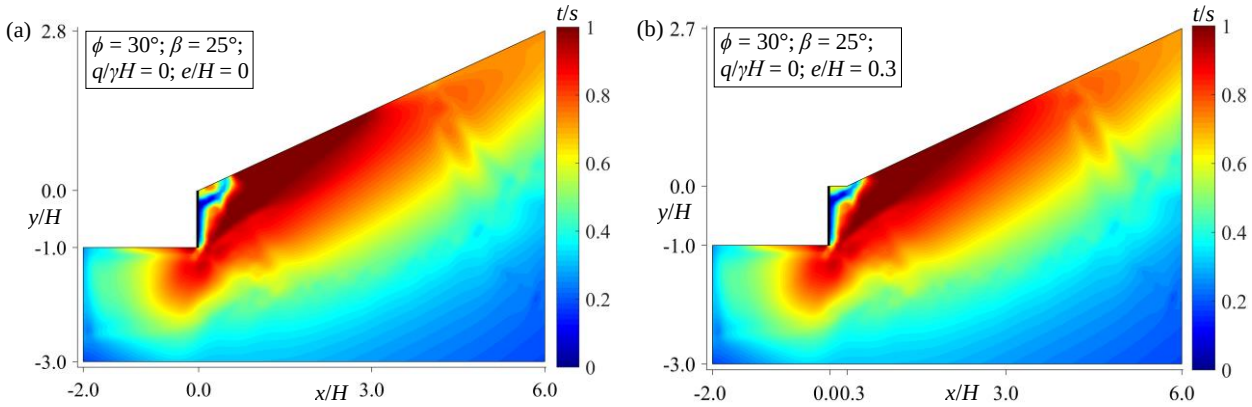

Fig. 8 For infinite height of slope, proximity of stress state to failure for $\phi = 30º$, $\beta = 25°$ and $q/\gamma H = 0$ with (a) $e/H = 0$; and (b) $e/H = 0.3$

equilibrium method for various combinations of wall friction angle (δ) and backfill slope angle (β). Similarly, the results by Sahoo and Ganesh (2018) using the upper bound theorem of limit analysis with composite collapse mechanism have been compared. From Fig. 11(b), it can be seen that the results of the present study are consistent with the previous studies, both experimental and analytical findings. The present solutions corresponding to $\beta = 0$ for horizontal ground surface and corresponding to $e/H = 0$ for different values of β in the case of sloping surface are also compared with upper bound limit analysis solutions of Soubra and Mauch (2002).

6. Conclusions

Finite element lower bound limit analysis solutions have been produced for estimating the active earth thrust on vertical walls retaining sandy sloping ground. The influence of slope toe position from the wall, height and angle of slope, frictional angle of sand, and surcharge load on the ground surface on the active earth force was investigated.

The following specific conclusions can be drawn from the present study.

- The magnitude of active earth thrust on a retaining wall supporting soil with a sloping surface becomes the same as that of retained ground with the horizontal surface when the location of the slope toe exceeds a certain distance from the wall, i.e., the critical toe distance.
- The magnitude of active thrust remains constant and the same as that of the infinite height of sloping ground when the height of sloping ground reaches a certain maximum value, i.e., critical slope height behind a retaining wall.
- The critical toe distance and slope height reduce with an increase in the values of soil friction angle, whereas they increase with the increase in the values of slope angle and ground surcharge.
- The changes in the critical toe distance have been noticed to be insignificant with changes in the height of sloping ground.
- The magnitudes of active earth force are higher for lower values of frictional soil angle, and for higher values of slope angle and surcharge on the ground.

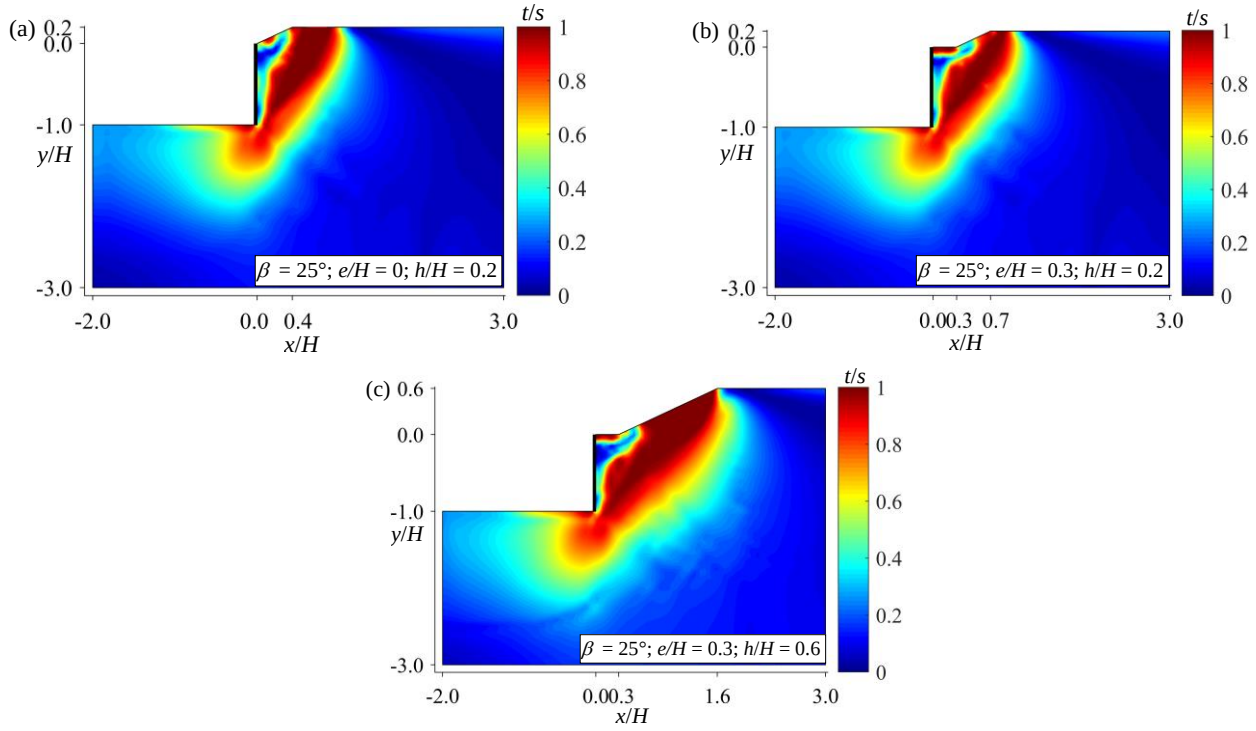

Fig. 9 For finite height of slope, proximity of stress state to failure for $\phi = 30^o$, $\beta = 25°$. and $q/\gamma H = 0$ with (a) $e/H = 0$, $h/H = 0.2$, (b) $e/H = 0.3$, $h/H = 0.2$; and (*c*) $e/H = 0.3$, $h/H = 0.6$

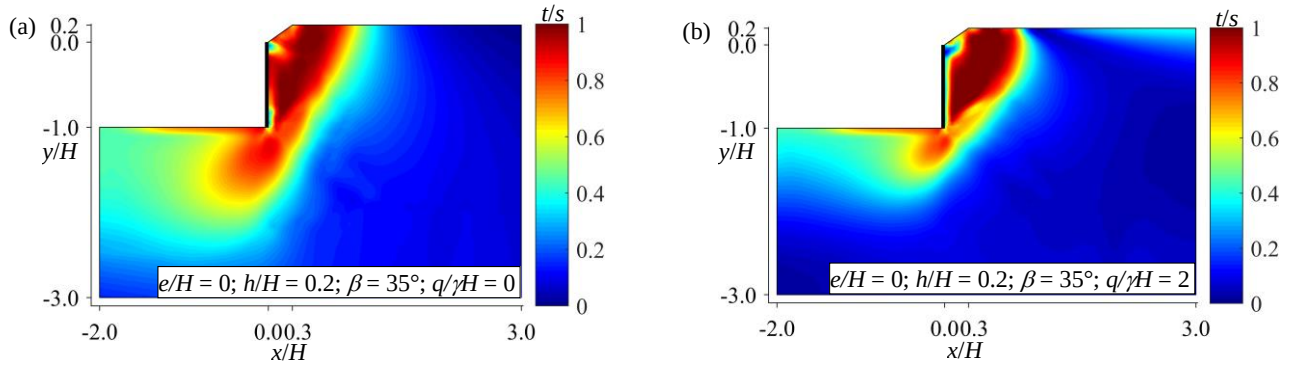

Fig. 10 For finite height of slope, proximity of stress state to failure for $\phi = 40^o$, $e/H = 0$ and $h/H = 0.2$ with (a) $\beta = 35°$, $q/\gamma H = 0$; and (b) $\beta = 35°$, $q/\gamma H = 2$

- The results enable the effective design of retaining walls in sloping terrains by quantifying critical toe distances and slope heights while providing reliable pressure coefficients for varying soil friction angles, slope inclinations, and surcharge load

References

Benmeddour, D., Mellas, M., Frank, R. and Mabrouki, A. (2012), "Numerical study of passive and active earth pressures of sands", *Comput. Geotech.*, **40**, 34-44. https://doi.org/10.1016/j.compgeo.2011.10.002.

Chen, W.F. and Rosenfarb, J.L. (1973), "Limit analysis solutions of earth pressure problems", *Soils Found.*, **13**(4), 45-60. https://doi.org/10.3208/sandf1972.13.4_45.

Coulomb, C.A. (1776), "Essai sur une application des regles des maximis et minimis a` quelques problemes de statique relatifs a l'arquiteture", Memoirs Academie Royal Pres. Division Sav. 7, Paris, France.

Drucker, D.C. (1953), "Limit analysis of two and three dimensional soil mechanics problems", *J. Mech. Phys. Solids*, **1**(4), 217-226. https://doi.org/10.1016/0022-5096(53)90001-5.

Fan, C.C. and Fang, Y.S. (2010), "Numerical solution of active earth pressures on rigid retaining walls built near rock faces", *Comput. Geotech.*, **37**(7-8), 1023-1029. https://doi.org/10.1016/j.compgeo.2010.08.004.

Fang, Y., Chen, J. and Chen, C. (1997), "Earth pressures with sloping backfill", *J. Geotech. Geoenviron. Eng.*, **123**(3), https://doi.org/10.1061/(ASCE)1090-0241(1997)123:3(250).

Greco, V.R. (2005), "Active earth thrust by backfills subject to a line surcharge", *Can. Geotech. J.*, **42**(5), 1255-1263. https://doi.org/10.1139/t05-038.

Greco, V.R. (2006), "Active thrust due to backfill subject to lines

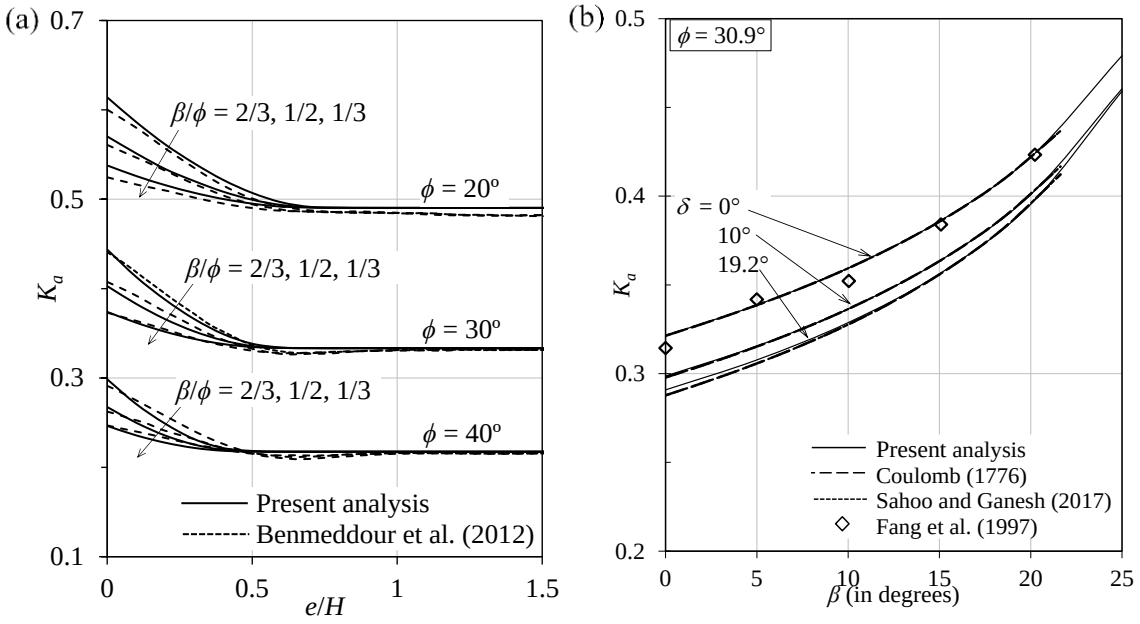

Fig. 11 A comparison of present results with the results obtained by (a) Benmeddour *et al*. (2012); and (b) Coulomb (1776), Sahoo and Ganesh (2017) and the experimental results reported by Fang *et al*. (1997) for ϕ = 30.9° and δ = 0°

of surcharge", *J. Geotech. Geoenviron. Eng*., **132**(2), 269-271. https://doi.org/10.1061/(ASCE)1090-0241(2006)132:2(269).

Greco, V.R. (2013), "Active thrust on retaining walls of narrow backfill width", *Comput. Geotech*., **50**, 66-78. https://doi.org/10.1016/j.compgeo.2012.12.007.

Jumikis, A.R. (1962), "Active and passive earth pressure coefficient tables (No. 43)", College of Enginering, Bureau of Engineering Research.

Kerisel, J. and Absi, E. (1990), "Active and passive earth pressure tables", Balkema, Rotterdam, The Netherlands.

Lai, F., Yang, D., Liu, S., Zhang, H. and Cheng, Y. (2022), "Towards an improved analytical framework to estimate active earth pressure in narrow $c-\phi$ soils behind rotating walls about the base", *Comput. Geotech*., **141**, 104544. https://doi.org/10.1016/j.compgeo.2021.104544.

Makrodimopoulos, A. and Martin, C.M. (2006), "Lower bound limit analysis of cohesive frictional materials using second-order cone programming", *Int. J. Numer. Meth. Eng*., **66**, 604–634. https://doi.org/10.1002/nme.1567.

MATLAB (2019), The MathWorks, Inc., Natick, Massachusetts, United States.

MOSEK, A. (2015), The MOSEK optimization toolbox for MATLAB manual. Version 7.1 (Revision 28).

Motta, E. (1994), "Generalized Coulomb active-earth pressure for distanced surcharge", *J. Geotech. Eng*., **120**(6), 1072-1079. https://doi.org/10.1061/(ASCE)0733-9410(1994)120:6(1072).

Rankine, W.J.M. (1857), "On the stability of loose earth", *Philos. Trans. Royal Soc., London*, **147**, 9-27. https://doi.org/10.1098/rstl.1857.0003.

Sahoo, J.P. and Ganesh, R. (2017), "Kinematic limit analysis approach for seismic active earth thrust coefficients of cohesive-frictional backfill", *Int. J. Geomech*., **18**(1), 04017123. https://doi.org/10.1061/(ASCE)GM.1943-5622.0001030.

Sloan, S.W. (1988), "Lower bound limit analysis using finite elements and linear programming", *Int. J. Numer. Anal. Meth. Geomech*., **12**, 61-77. https://doi.org/10.1002/nag.1610120105.

Soubra, A.H. and Macuh, B. (2002), "Active and passive earth pressure coefficients by a kinematical approach", *Proc. Inst. Civil Eng. Geotech. Eng*., **155**(2), 119-131. https://doi.org/10.1680/geng.2002.155.2.119.

Terzaghi, K. (1943), *Theoretical Soil Mechanics*. 5th ed., John Wiley & Sons Inc., New York, N.Y.

Yang, M. and Tang, X. (2017), "Rigid retaining walls with narrow cohesionless backfills under various wall movement modes", *Int. J. Geomech*., **17**(11), 04017098. https://doi.org/10.1061/(ASCE)GM.1943-5622.0001007.

CC